

Comparison between optically excited and electron-excited transitions above oxygen and nitrogen *K* edges in Cu_2O , O/Al , O/Ni , SiO_2 , and Si_3N_4

F. Della Valle,* G. Comelli, F. Zanini, and R. Rosei*

Dipartimento di Fisica, Università degli Studi di Trieste, via A. Valerio 2, I-34127 Trieste, Italy

G. Paolucci*

International School for Advanced Studies (ISAS), strada Costiera 11, I-34014 Trieste, Italy

(Received 10 September 1987; revised manuscript received 18 April 1988)

We compare transitions observed in photoabsorption spectra above the oxygen and nitrogen *K* edges in several compounds and chemisorption systems with transitions excited by the process of electron-energy loss detected in the reflection mode. We find few but significant discrepancies between the two, mainly attributable to quadrupole transitions and double inelastic scattering in the electron-energy-loss spectra. The problem of the extraction of structural information from the measurements is considered.

I. INTRODUCTION

The extended x-ray-absorption fine-structure (EXAFS) technique has been known for several years as a powerful method for the determination of geometries around a selected type of atom.¹ The extended fine structures above a core photoabsorption edge (typically the *K* edge) is interpreted in terms of backscattering of the excited photoelectron from the atoms surrounding the absorber, and the local geometry can be determined (after background subtraction) by Fourier transforming the spectrum or by using other computing techniques.¹ Because of the extended photon-energy range required (typically ≥ 400 eV) and of the weakness of the fine structures, most of the work performed up to now in this field used synchrotron radiation as a light source.

Several groups have developed techniques in which the excitation of the core level is obtained by using electrons rather than photons: appearance-potential spectroscopy (APS),² Auger-monitored extended energy-loss fine structure (AMEFS),³ extended energy-loss fine structure (EXELFS),⁴ and surface-extended energy-loss fine structure (SEELFS).⁵ We will focus our attention on EXELFS and SEELFS. In both cases an electron-energy-loss (EEL) spectrum is measured, but for EXELFS the experiment is performed in the transmission mode and for SEELFS in the reflection mode. In the latter case a high sensitivity to the surface is obtained. The analysis is carried out following the same procedure used in the EXAFS technique and this is usually justified by assuming that the experiments are performed in the high-energy and low-momentum-transfer limit, where optical dipole selection rules are applicable. This is certainly true for EXELFS but could be not completely true for SEELFS.^{6,7} Moreover, double losses will also play a role in an EEL experiment.

Up to now, most of the SEELFS papers which have appeared in the literature deal with low-energy edges (typically the M_{23} edge in the first-row transition metals⁵) lying in the (50–100)-eV range, and in these cases a good

agreement is found between x-ray absorption (XRA) and SEELFS, but no extensive studies have been performed on deeper edges, such as oxygen and nitrogen *K* edges. These atoms are very important in chemisorption studies and this should be a very promising field in which to apply the technique because of its surface sensitivity. On the other hand, it is important to check the applicability of the technique to these edges because their higher energy is expected to give two sorts of problems: a lower cross section (low signal) and a higher momentum transfer (nondipole selection rules).

In order to check whether these are real limitations of the technique, we have selected some oxygen and nitrogen compounds and chemisorption systems and compared XRA spectra taken from the literature with EEL spectra measured by us. We focused our attention on the near-edge structures up to about 200 eV above the edge. For this reason and for the sake of clarity we will refer to this spectroscopy as reflection ionization loss spectroscopy (RILS) in order to distinguish it from SEELFS. The materials we studied are Cu_2O , O/Al , O/Ni , SiO_2 , and Si_3N_4 .

In Sec. II we briefly discuss the mechanism of the EEL process and its theory. In Sec. III we will describe the experimental procedure. The results will be presented in Sec. IV and discussed in Sec. V.

II. THE ENERGY-LOSS PROCESS: THE OPTICAL LIMIT

The EEL process is usually described in terms of the Bethe theory.⁸ The starting point of the theory, which is based on the first-order perturbation theory (or first Born approximation), is that the primary energy E_p is much higher than the binding energy of the electron which is excited. This implies that the Bethe theory is not applicable to threshold spectroscopies, such as APS or AMEFS. Experimentally, the application of the Bethe theory is found to be justified whenever the primary energy is higher than approximately 4 times the energy loss

E_l .⁹ This is always the case for EXELFS but can be not true for SEELFS because an extended energy-loss range is required.

Within the validity of the Bethe theory, optical (dipole) selection rules can be applied in the low-momentum-transfer limit. In fact, the transition probability is given by

$$M_{if} = (A/q^3) |\langle f | \exp(i\mathbf{q}\cdot\mathbf{r}) | i \rangle|^2, \quad (1)$$

where A is a coefficient which depends on the geometry, \mathbf{q} is the momentum transfer, and $|f\rangle$ and $|i\rangle$ are the final and initial states, respectively. The exponential in (1) can be expanded to get

$$\exp(i\mathbf{q}\cdot\mathbf{r}) = 1 + i\mathbf{q}\cdot\mathbf{r} - \frac{1}{2}(\mathbf{q}\cdot\mathbf{r})^2 + O((\mathbf{q}\cdot\mathbf{r})^3). \quad (2)$$

The first term in (2) always gives a null contribution to (1) because of the orthogonality of the wave functions, the second term is the dipole term, and the third gives quadrupole transitions. If Russel-Saunders coupling is a good approximation, the selection rule given by the second term is the usual $\Delta l = \pm 1$, while the third term describes transitions with $\Delta l = 0 \pm 2$. The expansion (2) can be truncated to the second term if $\mathbf{q}\cdot\mathbf{r}$ is small compared to unity in the range over which the product of the wave functions in (1) is significantly different from zero. Since in the present case $|i\rangle$ is a localized state and $|f\rangle$ is a state in the continuum (a band in a solid), the first one will determine the r range. A rough estimate of the range of q for which the dipole approximation is valid for 1s levels of light elements is given by

$$qr_{1s} \approx qa_0/Z \ll 1, \quad (3)$$

where r_{1s} is the radius of the 1s wave function, $a_0 = \hbar^2/me^2$ is the Bohr radius, and Z is the atomic number.

For a given geometry and excitation energy, the evaluation of q is fairly easy if a single-scattering event is assumed. With the symbols of Fig. 1, one gets

$$q^2 = 2m/\hbar^2 \{ 2E_p [1 - (1 - E_l/E_p)^{1/2} \cos\theta] - E_l \}.$$

Therefore,

$$q_{\min} = [(2m/\hbar^2)E_p]^{1/2} [1 - (1 - E_l/E_p)^{1/2}] \quad (4a)$$

and

$$q_{\max} = [(2m/\hbar^2)E_p]^{1/2} [1 + (1 - E_l/E_p)^{1/2}] \quad (4b)$$

are the limits for the momentum-transfer range.

The single-scattering description predicts the experimental results only in the gas phase and in transmission experiments in solids, and even in those cases it fails at large-angle scattering,¹⁰ when the probability of detecting double-scattering events (a low- q inelastic collision followed or preceded by a high- q elastic one) gets very high. As pointed out in Ref. 11, the cross sections for $1s \rightarrow 1s$ (elastic scattering), $1s \rightarrow 2s$, and $1s \rightarrow 2p$ transitions in atomic hydrogen decrease as q^{-4} , q^{-12} , and q^{-14} , respectively, at high q . The effect of double scattering is that in a reflection experiment the momentum transferred during the loss processes which are detected is roughly given by

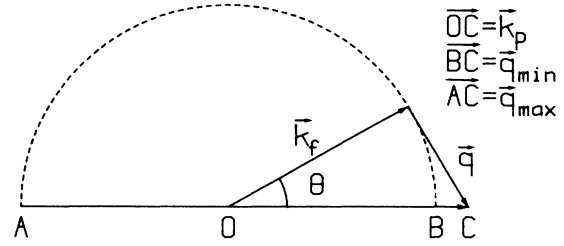


FIG. 1. Schematic diagram of the scattering process for a given energy loss E_l : $\mathbf{k}_p = [(2m/\hbar^2) \cdot E_p]^{1/2} \hat{\mathbf{k}}_p$ is the momentum of the electron impinging with energy E_p ; $\mathbf{k}_f = [(2m/\hbar^2)(E_p - E_l)]^{1/2} \hat{\mathbf{k}}_f$ is the momentum of the electron scattered to an angle θ , \mathbf{q} is the momentum transfer, q_{\min} and q_{\max} being its minimum and maximum values. The figure is scaled for $E_l = 500$ eV and $E_p = 2000$ eV.

the most probable q for a given energy loss. This means q_{\min} , as shown in Ref. 5 and verified experimentally in Ref. 7(a). Note that q_{\min} increases with E_l [Eq. (4a)]. Double scattering also implies the possibility of double-loss processes (see below).

From the above discussion it appears that in a RILS experiment it is important to know q_{\min} at the edge because this will give an idea of the applicability of the dipole (optical) selection rule. For the oxygen K edge ($E_l \approx 530$ eV) and $E_p = 2000$ eV, a typical primary energy for a RILS experiment, one gets

$$q_{\min} \approx 3 \text{ \AA}^{-1}$$

and

$$q_{\min} r_{1s} \approx 0.2.$$

Condition (3) is not fulfilled and therefore the dipole selection rule is not expected to hold in this case.

The nonapplicability of the dipole selection rule is supported, for example, by the gas-phase results of Hitchcock and Brion¹² for the excitation of Ne K shell ($E_l = 870$ eV) with $E_p = 2.5$ keV. Their experiment was performed in forward scattering, and therefore the momentum transfer was $q_{\min} = 4.9 \text{ \AA}^{-1}$. In these conditions they do observe the dipole-forbidden $1s \rightarrow 3s$ transition with an intensity of $\frac{1}{17}$ of the $1s \rightarrow 3p$ transition. A rough estimate of this ratio based on a calculation for the hydrogen atom reported in Ref. 8 gives a value of $\sim \frac{1}{30}$. Similar effects can be seen in most of the published SEELFS results on p edges; for example, the M_{23} of transition metals. In these cases, according to dipole selection rules, the M_1 level should not be seen, having the final state predominantly d character, and in fact it is much weaker in XRA than in RILS.¹³ This does not necessarily imply that structural information extracted from such spectra will be affected by the nondipole character of the spectra.¹⁴

III. EXPERIMENT

The EEL spectra reported here have been obtained using a standard Leybold-Heraeus ESCA system equipped

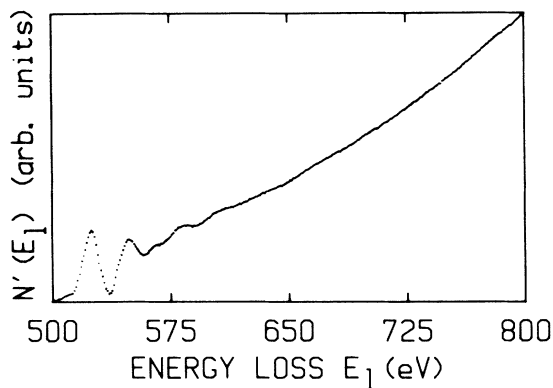


FIG. 2. First-derivative electron yield for 100 L oxygen on Ni{100}. The primary energy is 1700 eV, modulated by 10 V peak to peak.

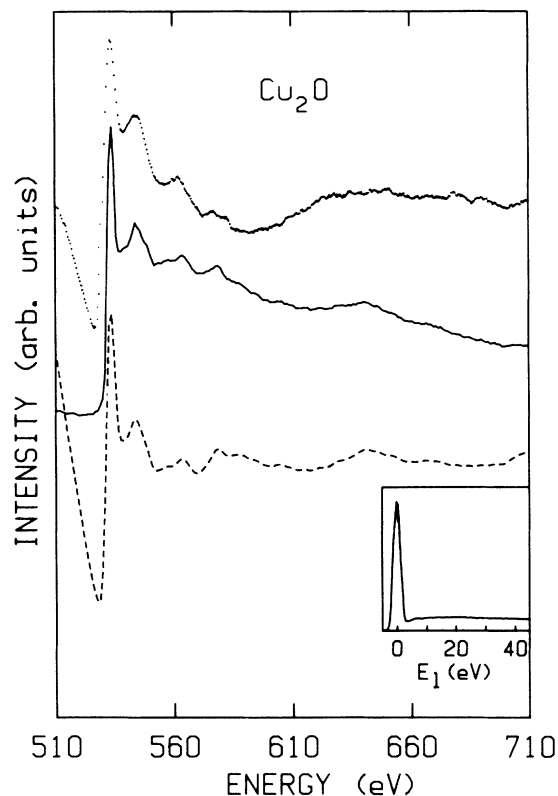


FIG. 3. Oxygen *K*-edge spectrum measured on polycrystalline Cu_2O by electron RILS (dots), compared with the corresponding XRA spectrum (solid line) (Ref. 19), and the convolution (dashed line) of the latter with the valence-band EEL spectrum shown in the inset. The abscissa is energy loss for the RILS spectrum and photon energy for the optical one. The primary energy for the RILS spectrum is 1850 eV, modulated by 10 V peak to peak; the spectrum was recorded in the first-derivative mode and has been integrated after trend removal. A background has been subtracted also from the convoluted spectrum. In the inset only the first 45 eV after the elastic peak are shown because the spectrum is structureless up to 200 eV. The primary energy for the valence-band spectrum is 1200 eV.

with a concentric hemispherical analyzer (EA10/100). Electrons from an Auger gun impinged on the sample surface with an angle of incidence of 60° , and were collected in a 6° cone around the surface normal. Because of the very low signal-to-background ratio (at most 10^{-3} for the edge jump), it has been necessary to operate the electronics in the analog first-derivative mode. The modulating voltage was not applied to the analyzer, as in ordinary Auger work, but to the primary energy in order to reduce spurious features such as Auger peaks and analyzer effects. The modulation used was 10 V peak to peak. The time required to record one spectrum was of the order of 10 h. The data acquisition was controlled by a microcomputer. The first-derivative spectra were integrated after background subtraction and compared to the optical ones. An example of a typical first-derivative spectrum is given in Fig. 2. It can be seen that for energy losses higher than 200 eV above the edge it is hard to distinguish true EXAFS-like oscillations from fluctuations of the background. The primary beam energy was in the range 1500–2000 eV. The electron beam was deliberately defocused in order to reduce the current density—i.e., the electron-beam damage—on the measured area of the sample. The signal did not decrease significantly in this

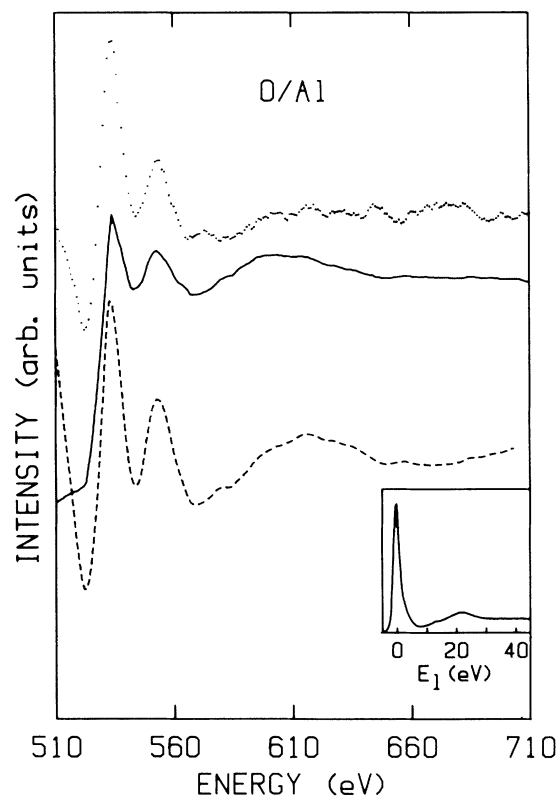


FIG. 4. Same as Fig. 3, but for 100 L oxygen on Al. XRA spectrum from Ref. 20. The primary energy for the RILS spectrum is 1600 eV. The primary energy for the valence-band spectrum is 1500 eV.

experimental condition since the electron analyzer we were using is designed to work with the large spot of unmonochromatized x-ray sources.

The samples have been prepared using procedures known from the literature: Cu_2O was prepared by exposing a pure polycrystalline Cu sample to air at 600 K and by heating it in vacuum to 1000 K, O/Al and O/Ni were prepared by exposing a polycrystalline Al foil and a Ni{100} surface to 100 L (1 L=1 langmuir, or 10^{-6} Torr sec) of O_2 which gives, respectively, about 1 monolayer coverage¹⁵ and 2–3 NiO layers¹⁶; SiO_2 was thermally grown on Si{111}; nonstoichiometric silicon nitride was formed by glow discharge; in the following we shall refer to it as Si_xN_y ; the measured concentration ratio y/x is 1.2.¹⁷ In all cases the cleanliness and the nature of the compounds were verified by XPS and Auger spectroscopy after each measurement in order to check for possible changes in the chemical composition or in the oxidation state. In particular, we monitored the Auger line of Si at 78 eV in SiO_2 , which is known to be sensitive to electron-beam damage.¹⁸ We found no significant change.

IV. RESULTS

In Fig. 3 we show the oxygen *K*-edge RILS spectrum of Cu_2O (top spectrum) compared with the XRA spectrum (second spectrum; see below for the explanation of the other spectra in Fig. 3). The overall resemblance of the two is rather evident: the features appear to be in the same energy position in both cases. It should be noted, however, that all the features are broader in the energy-loss spectrum. This cannot be explained by a poorer resolution in the RILS case, since the edge jump width is similar in the two spectra, and in our case the resolution was kept constant over the whole spectrum.

A similar behavior is found in the case of O/Ni and O/Al (Figs. 4 and 5).

The situation is different for the two silicon compounds. In SiO_2 (Fig. 6) a feature (labeled *B*) appears in the RILS spectrum which is not present in the XRA one. In Si_xN_y only a restricted energy range could be measured because of problems with charging of the sample. We show the spectrum in Fig. 7 together with the XRA one. The agreement between the two techniques is very poor for this compound: in particular, the feature labeled

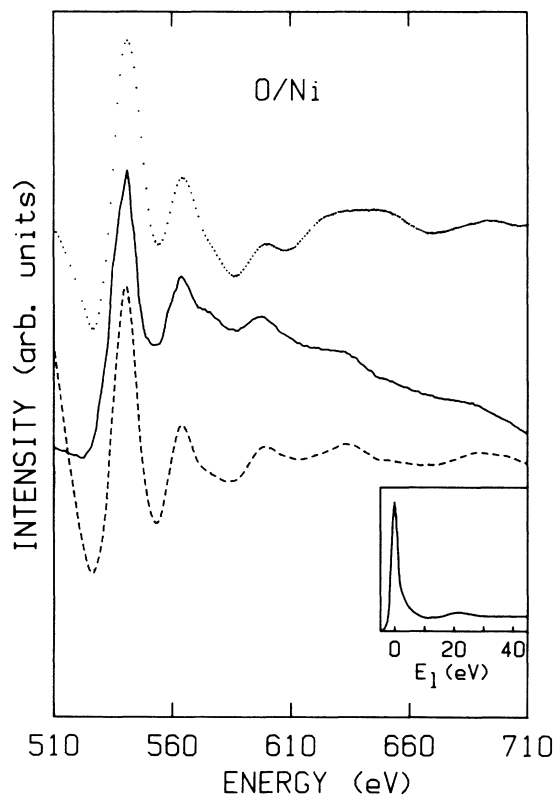


FIG. 5. Same as Fig. 3, but for 100 L oxygen on Ni{100}. XRA spectrum from Ref. 21. The primary energy for the RILS spectrum is 1700 eV. The primary energy for the valence-band spectrum is 1800 eV.

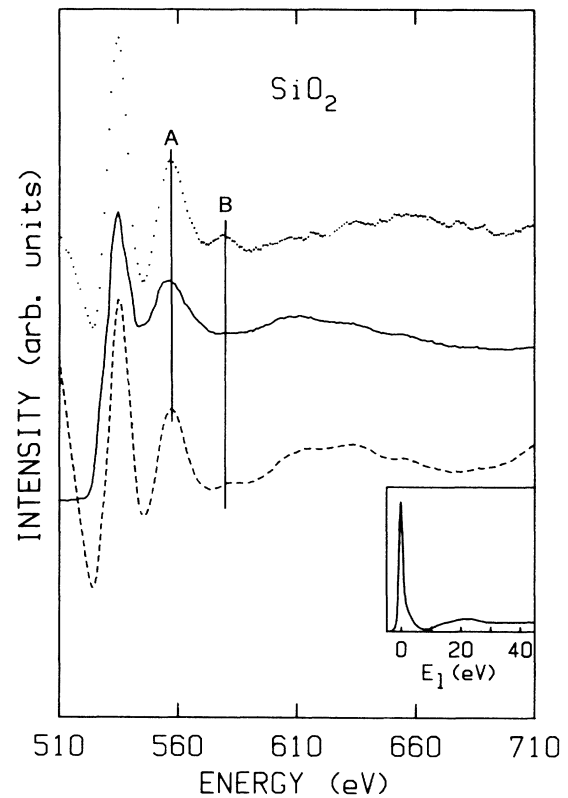


FIG. 6. Same as Fig. 3, but for SiO_2 grown on Si{111}. XRA spectrum from Ref. 22. The primary energy for the RILS spectrum is 1700 eV. The primary energy for the valence-band spectrum is 1600 eV.

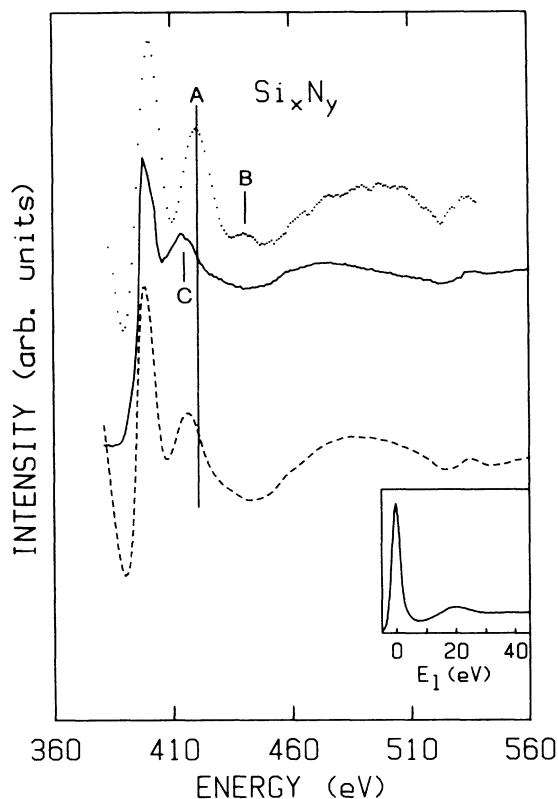


FIG. 7. Same as Fig. 3, but for the nitrogen K edge in polycrystalline Si_3N_4 . XRA spectrum from Ref. 22. The primary energy for the RILS spectrum is 1500 eV. The primary energy for the valence-band spectrum is 1500 eV.

A appears to be shifted by about 6 eV and the feature B is not present in the optical spectrum. XRA measurements on these two samples were repeated, and spectra identical to those reported in the literature were obtained.²³

V. DISCUSSION

Because of the experimental procedure adopted, and of the Auger and XPS checks after each measurement, we can rule out the possibility that the observed differences of RILS and XRA in the spectra of the two silicon compounds can be due to damage induced by the electron beam. We have already noted that in an optical-absorption measurement the momentum transfer is very small and therefore the usual dipole selection rules are obeyed; in a RILS experiment this is not true. The fact that double scattering can occur is also a complication because either or both scattering processes can be inelastic. The two effects (high momentum transfer and double scattering) must be taken into account when analyzing the data. Their weight relative to dipole transitions depends both on the experimental conditions (geometry and E_p) and on the electronic properties of the sample under study. We have already discussed the effect of the experimental conditions on the matrix element. A complete

evaluation of the quadrupole contributions cannot be made if the density of empty states is not taken into account.

Consider peak A in the Si_xN_y spectrum. It can be explained in terms of quadrupole transitions since a strong broad peak centered at about 26 eV above the edge is observed in the optically excited Si $2p$ edge spectrum (mainly involving d -like final states) in Si_3N_4 .²⁴ We think therefore that in this case quadrupole transitions completely mask the dipole contribution in peak A . On the other hand, we cannot explain features B in the spectra of this compound and of SiO_2 by this reasoning, since no high density of s or d states is expected at these energies for the two compounds.²⁴ The double-loss process is the other candidate.

In the inset of Fig. 7 the valence-band EEL spectrum of Si_xN_y is shown. A strong plasmon is present at about 20 eV and can be responsible for peak B . That is to say, primary electrons scattered at the energy of peak A can undergo a second loss process exciting electrons in the valence band of the solid and giving rise to peak B . This approach can as well explain peak B in the SiO_2 spectrum (see the inset of Fig. 6). In fact, this structure is at the right energy to be a plasmon replica of peak A .

In order to check for the consequences of this principle, we performed the convolution of each optical spectrum with an EEL valence-band spectrum recorded for this purpose (insets in Figs. 3–7). In other words, we treated each electron which has lost the energy E_l as a primary electron for valence-band excitations. It should be noted, however, that the exact weight of double-loss processes in EEL experiments cannot be simply inferred from the relative strength of the plasmon peak with respect to the primary peak in a valence-band spectrum. We want just to mention that the presence of double

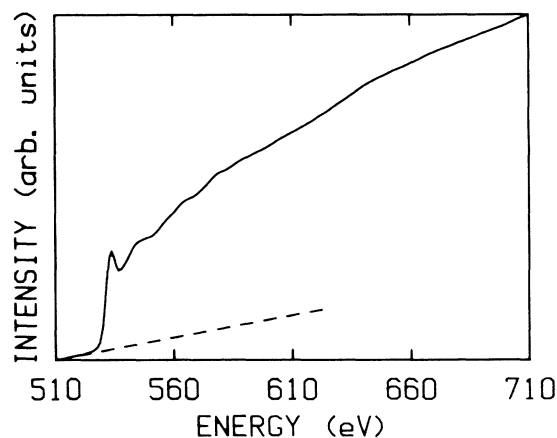


FIG. 8. Convolution of the Cu_2O XRA spectrum taken from Ref. 19 and shown in Fig. 3 and the valence-band EEL spectrum shown in the inset of the same figure. Note the different slope of the spectrum before (dashed line) and after the edge; this change in slope is to be compared with the behavior of the background in the original XRA spectrum.

losses is responsible for the fact that the slope of the background of RILS spectra recorded in the count mode increases after the edge,^{23,25} as in our simulation (Fig. 8).

For Cu₂O, O/Al, and O/Ni the convolution does not introduce extra features (third spectra in Figs. 3–5), but rather decreases the resolution, bringing the XRA spectra in closer agreement with the RILS ones. For SiO₂ (Fig. 6) a small peak appears at the same energy of peak *B* in the RILS spectrum, supporting our interpretation of this latter feature as arising from double-loss processes. For Si_xN_y (Fig. 7) the convolution fails to give rise to any plasmon replica in the XRA spectrum. This can be due to the fact that peak *C* in the XRA spectrum is not as pronounced as peak *A* in the RILS spectrum, and therefore its replica could fall below the detectability limit. In any case, this replica, in the convoluted spectrum, is to be looked for at any energy about 6 eV smaller than that of peak *B* (plasmon replica of peak *A*), since it originates from peak *C*, which is shifted by that amount from peak *A*. However, the agreement, also for the first four systems, is still not perfect. This has two possible origins. One is that the approximation of performing the convolution is rather crude; for instance, it is not taken into ac-

count that the geometry for plasmon excitation by an electron coming from the outside is different from the one in which the electron has already been scattered. Another possible source of discrepancies is given by the increased weight that quadrupole transitions can have in a RILS experiment with respect to XRA.

VI. CONCLUSIONS

Reflection ionization loss spectra above a core edge cannot be considered in principle identical to x-ray-absorption spectra. Effects like quadrupole transitions and plasmon replicas may occur that modify the simple dipole character of the observed peaks. Therefore we suggest great care in extracting structural information from this kind of measurement.

ACKNOWLEDGMENTS

We thank F. Evangelisti and P. Fiorini for having provided us with the Si_xN_y sample. We thank S. Modesti for continuous help and critical reading of the manuscript.

*Also at Centro Interuniversitario Struttura della Materia (CISM), P.le A. Moro 2, I-00185 Roma (Italy).

¹P. A. Lee, P. H. Citrin, P. Eisenberger, and B. M. Kincaid, *Rev. Mod. Phys.* **53**, 769 (1981), and references therein.

²T. L. Einstein, M. J. Mehl, J. F. Morar, R. L. Park and G. E. Laramore, in *EXAFS and Near Edge Structures*, edited by A. Bianconi, L. Incoccia and S. Stipcich (Springer, Berlin, 1983), p. 391.

³J. F. Morar and R. L. Park, *J. Vac. Sci. Technol. A* **1**, 1043 (1983).

⁴R. D. Leapman, L. A. Grunes, P. L. Fejes, and J. Silcox, in *EXAFS Spectroscopy—Techniques and Applications*, edited by B. K. Teo and D. C. Joy (Plenum, New York, 1981), p. 217.

⁵M. De Crescenzi and G. Chiarello, *J. Phys. C* **18**, 3595 (1985), and references therein.

⁶A. E. Meixner, R. E. Dietz, G. S. Brown, and P. M. Platzman, *Solid State Commun.* **27**, 1255 (1978); see also A. G. Nassiopoulos and J. Cazaux, *Surf. Sci.* **165**, 203 (1986).

⁷(a) J. Cazaux and A. G. Nassiopoulos, *Surf. Sci.* **162**, 965 (1985); (b) Y. U. Idzerda, E. D. Williams, T. L. Einstein, and R. L. Park, *ibid.* **160**, 75 (1985).

⁸M. Inokuti, *Rev. Mod. Phys.* **43**, 297 (1971).

⁹C. J. Powell, *Rev. Mod. Phys.* **48**, 33 (1976).

¹⁰G. E. Chamberlain, J. A. Simpson, S. R. Mielczarek, and C. E. Kuyatt, *J. Chem. Phys.* **47**, 4266 (1967).

¹¹L. Vriens, J. A. Simpson, and S. R. Mielczarek, *Phys. Rev.* **165**, 7 (1968).

¹²A. P. Hitchcock and C. E. Brion, *J. Phys. B* **13**, 3269 (1980).

¹³M. Fanfoni, S. Modesti, N. Motta, M. De Crescenzi, and R. Rosei, *Phys. Rev. B* **32**, 7826 (1985).

¹⁴T. Tyliczszak and A. P. Hitchcock, *J. Vac. Sci. Technol. A* **4**, 1372 (1986).

¹⁵S. A. Flodström, R. Z. Bachrach, R. S. Bauer, and S. B. M. Hagström, *Phys. Rev. Lett.* **37**, 1282 (1976).

¹⁶D. F. Mitchell, P. B. Sewell, and M. Cohen, *Surf. Sci.* **61**, 355 (1976).

¹⁷F. Evangelisti and P. Fiorini (private communication).

¹⁸S. Thomas, *J. Appl. Phys.* **45**, 161 (1974).

¹⁹U. Döbler, K. Baberschke, J. Haase, and A. Puschmann, *Phys. Rev. Lett.* **52**, 1437 (1984).

²⁰D. Norman, S. Brennan, R. Jaeger, and J. Stöhr, *Surf. Sci.* **105**, L297 (1981).

²¹J. Stöhr, *Jpn. J. Appl. Phys.* **17**, Suppl. 17-2, 217 (1978).

²²J. Stöhr, L. Johansson, I. Lindau, and P. Pianetta, *Phys. Rev. B* **20**, 664 (1979).

²³S. Modesti (unpublished).

²⁴F. C. Brown, R. Z. Bachrach, and M. Skibowski, *Phys. Rev. B* **15**, 4781 (1977).

²⁵A. Morgante, baccalaureate thesis (Laurea in Fisica), University of Trieste, 1985 (unpublished).